PCCP

PERSPECTIVE

View Article Online
View Journal | View Issue

Cite this: *Phys. Chem. Chem. Phys.*, 2014, **16**, 2200

Infrared spectra of free radicals and protonated species produced in *para*-hydrogen matrices

Mohammed Bahou,[a] Prasanta Das,[a] Yu-Fang Lee,[a] Yu-Jong Wu[b] and Yuan-Pern Lee*[ac]

Received 4th October 2013,
Accepted 29th November 2013

DOI: 10.1039/c3cp54184c

www.rsc.org/pccp

The quantum solid *para*-hydrogen (p-H_2) has emerged as a new host for matrix isolation experiments. Among several unique characteristics, the diminished cage effect enables the possibility of producing free radicals *via* either photolysis *in situ* or bimolecular reactions of molecules with atoms or free radicals that are produced *in situ* from their precursors upon photo-irradiation. Many free radicals that are unlikely to be produced in noble-gas matrices can be produced readily in solid p-H_2. In addition, protonated species can be produced upon electron bombardment of p-H_2 containing a small proportion of the precursor during deposition. The application of this novel technique to generate protonated polycyclic aromatic hydrocarbons (PAH) and their neutral counterparts demonstrates its superiority over other methods. The technique of using p-H_2 as a matrix host has opened up many possibilities for the preparation of free radicals and unstable species and their spectral characterization. Many new areas of applications and fundamental understanding concerning the p-H_2 matrix await further exploration.

1. Introduction

The matrix isolation technique involves condensation of a mixture of an inert gas (termed "host") containing a small proportion of a species of interest (termed "guest") onto a substrate maintained at low temperature. Since its inception in 1954, the matrix-isolation technique has served as a powerful method to trap reactive chemical species, especially free radicals, for diverse spectral characterizations.[1–5] Spectral characterization of these reactive species isolated in matrices using infrared (IR) absorption has been commonly employed because of its ease of use and the structural information that can be obtained. Because the reactive species are stabilized in matrices at low temperature, typically no rapid transient detection is required. The absence of rotational lines and hot bands make the observed IR spectrum of matrix-isolated species much simplified compared to that in the gaseous phase. Matrix shifts for the vibrational wavenumbers of species in solid Ar and Ne from those in the gaseous phase are typically smaller than 1 per cent.[6] Because most of the sample is deposited onto the substrate during deposition, the amount of sample required is much smaller than that typically used in experiments using flowing gases; the use of isotopically substituted species and specially synthesized precursors becomes feasible.

The preparation of free radicals in inert-gas matrices by photolysis *in situ* might be difficult, however, because of the matrix cage effect. Because of the large barrier involved in exiting the site of production, the threshold of photodissociation in matrices is typically observed to be greater, and the photodissociation yield smaller, than those in the gaseous phase. As a result, upon photodissociation of precursors such as $CH_2CHC(O)Cl$ and CH_3SSCH_3, fragments Cl and CH_3S cannot escape from the original site, thus hampering the formation of isolated free radicals such as CH_2CHCO and CH_3S from photolysis of $CH_2CHC(O)Cl$ and CH_3SSCH_3, respectively.[7,8]

[a] *Department of Applied Chemistry and Institute of Molecular Science, National Chiao Tung University, 1001, Ta-Hsueh Road, Hsinchu 30010, Taiwan. E-mail: yplee@mail.nctu.edu.tw*
[b] *National Synchrotron Radiation Research Center, 101, Hsin-Ann Road, Hsinchu 30076, Taiwan*
[c] *Institute of Atomic and Molecular Sciences, Academia Sinica, Taipei 10617, Taiwan*

Yuan-Pern Lee

Yuan-Pern Lee received his PhD in chemistry from U. C. Berkeley in 1979 and has been a National Chair Professor in the Department of Applied Chemistry, Chiao Tung University, Taiwan, since 2004. His main research topics concern spectroscopy, kinetics, and dynamics of free radicals that are important in atmospheric, combustion, or planetary chemistry using diverse experimental methods including step-scan time-resolved FTIR (emission or absorption), matrix isolation using p-H_2, cavity ringdown, IR-VUV photoionization/time-of-flight mass detection, and transient absorption using ultrafast lasers.

In contrast, the matrix cage effect consequently increases the chances of forming various isomers of the precursor or other stable products, or their complexes, for which production in the gaseous phase might be difficult. Over the years, we have taken advantage of these characteristics and produced many new species such as HOONO,[9,10] *cyc*-CS_2,[11] and SOO (ref. 12) from photolysis of HNO_3, CS_2, and SO_2, respectively. Detailed accounts of applications of these types are found elsewhere.[13,14]

The emergent use of *para*-hydrogen (*p*-H_2) as a matrix host has generated great interest because some unique characteristics are associated with this quantum solid.[15–21] Because the amplitude of the zero-point lattice vibrations of *p*-H_2 is a substantial fraction of the spacing between nearest H_2 molecules, the matrix is considered to be 'soft', thus leading to a reduced inhomogeneous broadening of lines of the guest molecules;[22] spectral line widths as small as 0.008 cm^{-1} have been reported.[23,24] Associated with this softness is the diminished matrix cage effect of *p*-H_2. A few species such as CO (ref. 25 and 26), CH_4 (ref. 23 and 24), H_2O (ref. 27), and HCl (ref. 28) are reported to perform slightly hindered rotation in solid *p*-H_2. For larger species, the feasibility of internal rotation (torsion) and of rotation about a single axis has been reported for CH_3OH (ref. 29) and CH_3F (ref. 30), respectively; such rotations were not observed in noble-gas matrices.

The diminished cage effect of the *p*-H_2 matrix is of particular interest for the preparation of atoms or free radicals. For instance, the primary products upon photo-irradiation of Cl_2 in the presence of molecules such as CS_2 or OCS jointly isolated in noble-gas matrices have structures of the form ClC(=S)SCl or ClC(=O)SCl that contains two Cl atoms because, upon photodissociation of Cl_2, the two Cl atoms cannot escape from the original noble-gas matrix cage so that both Cl atoms react with CS_2 or OCS.[31–33] In contrast, Huang and Lee irradiated a *p*-H_2 matrix containing Cl_2 and CS_2 with laser emission at 340 nm and produced ClSCS.[34] Similarly, because an I atom is readily separable from the counter fragment, Momose and co-workers have demonstrated that CH_3 and C_2H_5 were produced, respectively, upon UV irradiation of CH_3I (ref. 35 and 36) and C_2H_5I (ref. 37 and 38) isolated in solid *p*-H_2. Such a practice is typically difficult in noble-gas matrices because of the cage effect.

This situation opens various possibilities for producing free radicals or unstable species on irradiation of a *p*-H_2 matrix containing appropriate precursors. Here we describe the recent advances in IR spectroscopy of free radicals or unstable species produced and isolated in solid *p*-H_2. We demonstrate that it is possible to produce free radicals using either photolysis *in situ* or various bimolecular reactions involving small molecules and atoms or radicals that are produced upon photolysis of precursors in solid *p*-H_2. We also describe a novel method of using *p*-H_2 to make protonated species and their neutral counterparts. Some limitations of preparation of free radicals in a *p*-H_2 matrix are also discussed.

2. Experiments and spectral assignments

Two methods are typically employed for *p*-H_2 matrix isolation. The method of rapid deposition uses a large rate of flow ($\sim$0.2 mol h^{-1}) of gases to condense onto a substrate maintained at $\sim$2 K, achieved by pumping liquid helium.[39] The advantages are the ability to form a thick transparent film of *p*-H_2 in a short period and the ability to perform experiments at temperature lower than 3 K. The disadvantages are the costly liquid helium consumption in the continuously pumping mode and the difficulty in performing experiments over an extended period.

The second method employs a commercial closed-cycle refrigerator that can cool the substrate from 298 K to $\sim$3 K within 1 h.[29] The continuous deposition method with slower flow rates, typically used in conventional matrix isolation experiments using a noble-gas host, is hence analogously employed. Although the initial investment of a closed-cycle refrigerator is high, subsequent operation is much more economical than using liquid helium, and experiments with extended periods are easy. The disadvantage of the closed-cycle refrigerator system is that the present lowest temperature achievable is $\sim$3 K, slightly higher than using liquid helium at decreased pressure. The lowest temperature achievable might be critical to some experiments such as those involving tunnelling reactions.

An additional closed-cycle refrigerator system capable of controlling the temperature in the range 10–25 K is required to convert *n*-H_2 to *p*-H_2. The method is well established: after passage through a trap at 77 K, H_2 (99.9999%) is passed through the *p*-H_2 converter before direct deposition or preparation of sample mixtures.[39–41] The *p*-H_2 converter comprises a copper cell filled with APACHI (a paramagnetic nickel salt supported on particulate silica gel) or hydrated iron(III) oxide catalyst and cooled using a closed-cycle refrigerator. The efficiency of conversion is controlled by the temperature of the catalyst; at 15 K the concentration of *o*-H_2 is typically $\sim$100 ppm according to the Boltzmann distribution.

Spectral assignments of unknown species are typically based on the expected photofragmentation and/or chemical reactions, comparison of observed vibrational wavenumbers and relative IR intensities with anharmonic vibrational wavenumbers and IR intensities predicted quantum-chemically, and, if possible, isotopic shifts. Secondary photo-irradiation, annealing, or maintaining the matrix over a prolonged period helps to sort observed lines into groups with distinct behaviour, likely associated with varied species.

3. Production of atoms and free radicals from photolysis *in situ*

Perhaps the simplest way to produce atoms and free radicals in solid *p*-H_2 is to photolyze precursors *in situ*. Because of the diminished cage effect, the fragments might separate and become isolated upon photodissociation. In contrast, for noble-gas matrices, the fragments are typically maintained in the original cage so that isolation of free radicals becomes infeasible.

Raston and Anderson photodissociated Cl_2 trapped in solid *p*-H_2 at 2 K with laser emission at 355 nm and reported the observation of isolated Cl atoms *via* an absorption line at

943.8 cm^{-1} associated with the spin–orbit transition $^2P_{1/2} \leftarrow {}^2P_{3/2}$ of Cl.[42] Similarly, Kettwich *et al.* studied the spin–orbit transition of the Br atom produced on UV photolysis of Br_2 isolated in solid *p*-H_2 and *o*-D_2;[43] the transition is enhanced eight-fold relative to the gas phase through interactions with the matrix.[44] The associated theory for the observed lines of Cl in *p*-H_2 has been developed by Hinde.[45,46] Momose has also investigated the spin–orbit transitions of the I atom.[47] One can use various absorption lines of the halogen atoms involving their spin–orbit transitions or halogen atom-induced absorptions of *p*-H_2 to monitor directly the concentration.

As an example for production of free radicals due to the mobility of Cl atoms in solid *p*-H_2, we compare the photolysis of acryloyl chloride, $CH_2CHC(O)Cl$, in solid Ar and *p*-H_2. Pietri *et al.* used light of wavelength ≥ 310 nm to photolyze $CH_2CHC(O)Cl$ in solid Ar at 10 K and observed IR absorption of only 3-chloro-1,2-propenone, $CH_2ClCHCO$, with a characteristic broad feature near 2139 cm^{-1}.[7] The formation of only $CH_2ClCHCO$ in this experiment is due to the matrix cage effect; upon C–Cl fission, the Cl fragment cannot escape from the original cage so the secondary reaction of Cl + C_2H_3CO yields $CH_2ClCHCO$. In contrast, Das and Lee irradiated, with laser light at 193 nm, a *p*-H_2 matrix containing $CH_2CHC(O)Cl$ at 3.2 K, and observed twelve IR absorption lines of the 3-propenonyl ($^{\bullet}CH_2CHCO$) radical, including the most intense feature of the C=O stretching mode at 2103.1 cm^{-1}.[48] The 3-propenonyl is the most stable isomer of the product from C–Cl bond fission.

Similarly, ClCS was observed from photolysis at 248 nm of Cl_2CS in solid *p*-H_2.[34] Irradiation at 239 ± 20 nm of a *p*-H_2 matrix containing methoxysulfinyl chloride, $CH_3OS(O)Cl$, and its per-deuterated isotopomer, $CD_3OS(O)Cl$, yields absorption lines of all 11 vibrational modes of CH_3OSO/CD_3OSO in the spectral region of detection,[49] extending the information of only four bands observed in the photolysis of gaseous $CH_3OS(O)Cl$ with a step-scan Fourier-transform infrared (ss-FTIR) spectrometer.[50]

As described in Section 1, CH_3 and C_2H_5 are two free radicals that Momose and coworkers reported to be produced from photolysis *in situ* of CH_3I and C_2H_5I, respectively. Further experiments led to analysis of rotational fine structures for ν_3 and ν_4 of CH_3 and CD_3,[51,52] which were subjected to further splitting due to the electrostatic field of solid *p*-H_2. Detailed analysis indicated that the rotational constants of the CD_3 radical are only slightly smaller than those in the gas phase. The determined crystal-field parameters indicated significant quantum effects in the intermolecular interactions between the radicals and dihydrogen molecules in solid *p*-H_2. Moreover, Miyamoto *et al.* produced chloromethyl (CH_2Cl) radical by UV photolysis *in situ* of chloroiodomethane (CH_2ICl) isolated in solid *p*-H_2.[53] Analysis of the vibration-rotational spectra revealed that the radical exhibited quantized one-dimensional rotational motion around the C–Cl bond, whereas the *ortho* and *para* nuclear spin species were clearly distinguishable in the spectra. The nuclear spin conversion between the *ortho* and *para* nuclear spin species of this radical in solid *p*-H_2 occurred on a time scale of a few hours at 3.6 K.

Ruzi and Anderson studied photolysis of NH_3 in solid *p*-H_2 *in situ* with light at 193 nm and detected NH_2 and NH products.[54] Interestingly, they detected the NH_2 radical only during UV irradiation; the NH_2 reacted rapidly with the *p*-H_2 host. A detailed analysis of the spectral lineshapes of these species revealed small changes to the vibrational wavenumbers, nearly free rotation, and that the splittings due to the unpaired electron spin were nearly the same as the values for the gaseous phase.

The 'escaped' fragment is not limited to only atoms; more complicated free radicals can also escape from the counter fragment upon photolysis. Bahou and Lee photodissociated three precursors CH_3SH, CH_3SCH_3 and CH_3SSCH_3 isolated in solid *p*-H_2 and observed IR absorption lines of CH_3S in all cases.[8] In contrast, photolysis of CH_3SSCH_3 isolated in solid Ar produced mainly H_2CS, CH_3SH and CS_2, but not CH_3S; the former two are produced from secondary reaction of CH_3S + CH_3S within the original matrix cage. This great contrast is illustrated in Fig. 1. Trace (a) shows the difference spectrum of CH_3SSCH_3/Ar obtained upon UV photolysis near 254 nm; lines of CH_3SH, H_2CS, and CS_2 are indicated. Trace (b) shows the difference spectrum of CH_3SSCH_3/*p*-H_2 obtained upon photolysis at 270 nm; lines of CH_3S are indicated with arrows. Before this work, no IR spectrum of CH_3S had been reported despite much effort to acquire it. The IR spectrum of CH_3S is complicated because it is subject to Jahn–Teller distortion and spin–orbit coupling. The identification of several fundamental and combination or overtone modes provided not only a way to directly probe CH_3S but also an effective test of the accuracy of quantum-chemical calculations of a Jahn–Teller molecule; the predicted vibrational wavenumbers are shown in Fig. 1(c).[55,56]

In some cases, several channels might take place upon UV excitation. Ruzi and Anderson reported IR spectra of the photodecomposition products of *N*-methylformamide ($HCONHCH_3$) isolated in solid *p*-H_2 at 1.9 K.[57] By studying the detailed photokinetics, they distinguished between primary and secondary

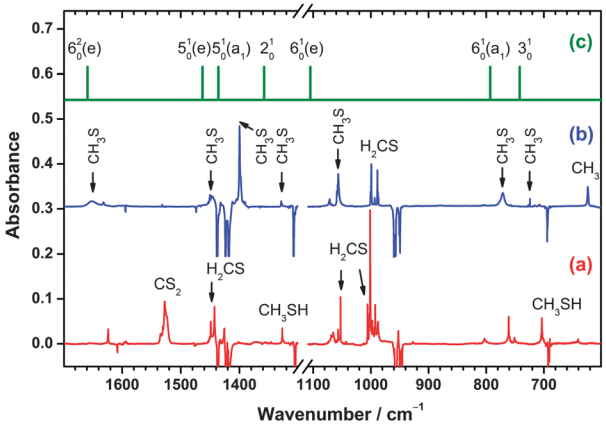

Fig. 1 Comparison of photolysis products of CH_3SSCH_3 in solid Ar and *p*-H_2. (a) Difference spectrum of CH_3SSCH_3/Ar (1/1000) upon photolysis with a medium-pressure Hg lamp and a band-pass filter at 254 nm for 8 h. (b) Difference spectrum CH_3SSCH_3/*p*-H_2 (1/1000) upon photolysis with a medium-pressure Hg lamp and a band-pass filter at 270 nm for 4 h; new features of CH_3S are indicated with arrows. (c) Quantum-chemically predicted line positions of CH_3S are shown as sticks; assignments are listed but no information on intensities was provided.[56] Traces (b) and (c) are displaced for viewing clarity.

photolysis products. Three competing primary dissociation channels – HCO + $NHCH_3$, H + $CONHCH_3$, and CO + CH_3NH_2 – with branching ratios of 0.46 : 0.032 : 0.51 were observed; the primary photolysis products $NHCH_3$ and $CONHCH_3$ were observed for the first time using IR spectroscopy.

4. Production of free radicals from photo-initiated bimolecular reactions

The production of free radicals in solid *p*-H_2 is not limited to photolysis *in situ*; the atom or radical produced upon photolysis can react further with another molecule, hence expanding the types of free radicals that can be prepared. The reaction can take place during irradiation or upon annealing of the irradiated *p*-H_2 matrix; the latter process is free from interference due to photo-excitation or secondary photodecomposition. In general, this scheme is feasible for barrierless reactions. If the reaction has a barrier, a competition between energy relaxation and reaction of the decomposition fragment needs to be considered. Energy relaxation in solid *p*-H_2 is typically rapid; hence a reaction with a barrier might be difficult to occur. For example, we irradiated a CH_3I/CO/*p*-H_2 (1/1/2000) matrix with light at 248 nm for 15 min followed by annealing of the matrix at 5.1 K for 2 min and observed only a complex of CH_3 with CO, as shown in trace (a) of Fig. 2. In contrast, when we photolyzed $CH_3C(O)Cl$/*p*-H_2 (1/2500) with light at 248 nm, we observed IR absorption lines of CH_3CO, as shown in trace (b) of Fig. 2; these lines agree satisfactorily with those predicted with the B3PW91/aug-cc-pVTZ method, as shown in trace (c). According to quantum-chemical computations, the barrier of the reaction $CH_3 + CO \rightarrow CH_3CO$ is 18–27 kJ mol^{-1}.[58] The experimental activation energy was determined to be 27.6 kJ mol^{-1}.[59] CH_3 has translational energy ~134 kJ mol^{-1} and internal energy ~42 kJ mol^{-1} upon photodissociation of CH_3I at 254 nm;[60] the former corresponds to translational energy ~87 kJ mol^{-1} for the reaction of CH_3 + CO in the centre-of-mass coordinate, greater than the barrier. Apparently the rapid quenching of CH_3 disabled this reaction.

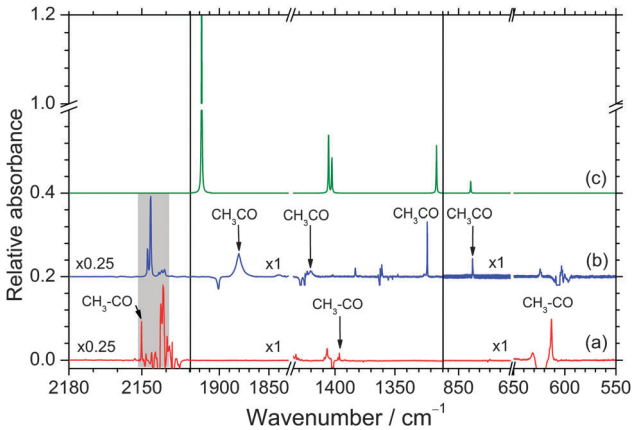

Fig. 2 Comparison of photolysis products in two matrix samples. (a) Difference spectrum of CH_3I/CO/*p*-H_2 (1/1/2000) upon photolysis at 248 nm for 15 min followed by annealing at 5.1 K for 2 min. (b) Difference spectrum of $CH_3C(O)Cl$/*p*-H_2 (1/2500) upon photolysis at 248 nm for 2 h. (c) IR spectrum of CH_3CO simulated according to anharmonic vibrational wavenumbers and IR intensities obtained with the B3PW91/aug-cc-pVTZ method. The region due to interference from absorption of ketene (CH_2=C=O) and CO is marked with grey. Traces (b) and (c) are displaced for viewing clarity.

We describe here IR spectra of free radicals produced from the reactions of Cl atom, CH_3 radical, and H atom with a second molecule.

4.1 Reactions of Cl atom

Because Cl atom is readily produced on photolysis of Cl_2 isolated in solid *p*-H_2 with light from an excimer laser (308 nm), a frequency-tripled Nd:YAG laser (355 nm), or a light-emitting diode (365 ± 10 nm), numerous free radicals involving reactions of Cl with a second molecule have been reported.

As described in Section 1, irradiation of a *p*-H_2 matrix containing Cl_2 and CS_2 at 3.3 K with laser emission at 340 nm followed by annealing of the matrix produced prominent features at 1479.5 and 1480.8 cm^{-1}, attributed to the ν_1 (SCS antisymmetric stretching) mode of ClSCS,[34] produced from the reaction Cl + CS_2. In contrast, ClC(=S)SCl was produced as the major product on irradiation of noble-gas matrices containing Cl_2 and CS_2.[31]

Upon irradiation at 365 nm of a Cl_2/C_5H_5N/*p*-H_2 matrix to generate Cl atom *in situ* and annealing at 5.1 K for 3 min to induce a secondary reaction, the 1-chloropyridinyl (C_5H_5N–Cl) radical was identified as the major product of the reaction Cl + C_5H_5N; absorption lines at 3075.9, 1449.7, 1200.6, 1148.8, 1069.3, 1017.4, 742.9, and 688.7 cm^{-1} were observed.[61] The observation of the preferential addition of Cl to the N-site of pyridine to form C_5H_5N–Cl radical over addition to the C-site to form 2-, 3-, or 4-chloropyridinyl (ClC_5H_5N) radicals is consistent with the quantum-chemical prediction that the formation of the former proceeds *via* a barrierless path with the least energy.[62]

The reaction of Cl atom with unsaturated hydrocarbons is important in atmospheric chemistry and organic synthesis. In the radical mechanism, the initial process involves addition of a Cl atom to the C=C bond to form chloroalkyl radicals, but the direct IR identification of these chloroalkyl radicals is unreported. We have investigated free-radical intermediates produced from the reactions of Cl atoms with C_2H_4,[63] propene (C_3H_6),[64] *trans*-1,3-butadiene (C_4H_8),[65] and benzene (C_6H_6).[66] In all cases, Cl atoms were produced on irradiation of Cl_2 in solid *p*-H_2 with light near 365 nm from a light-emitting diode. Some free radicals were produced immediately after photolysis of Cl_2; further production *via* bimolecular reactions with Cl was induced on annealing of the matrix briefly to ~5 K.

Irradiation at 365 nm of a *p*-H_2 matrix containing Cl_2 and C_2H_4 in small proportions produced new lines in the IR spectrum: an intense line at 664.0 cm^{-1} and weaker ones at 562.1, 1069.9, 1228.0, 3041.1, and 3129.3 cm^{-1} are assigned to the 2-chloroethyl ($^{\bullet}CH_2CH_2Cl$) radical.[63] Isotopic experiments with C_2D_4 and *t*-$C_2H_2D_2$ were performed and observation of IR lines due to the deuterated isotopomers $^{\bullet}CD_2CD_2Cl$ and $^{\bullet}C_2H_2D_2Cl$ further supported the assignments.

For the Cl + propene reaction, we observed only the 2-chloropropyl ($^{\bullet}CH_2CHClCH_3$) radical, not the 1-chloropropyl radical; an

intense line at 649.9 cm^{-1} and weaker ones at 1007.6, 1132.7, 1149.6, 1214.7, and 1382.2 cm^{-1} were observed.[64] This result indicates that the addition of the Cl atom to the C=C bond of propene occurred primarily at the central carbon atom, in sharp contrast to the generally accepted mechanism in organic chemistry as observed in the gaseous phase; the addition of Cl to the terminal carbon atom is energetically favoured there. This unique selectivity might be due to the steric effects in solid *p*-H_2, in which the complex of Cl_2 and propene are positioned so that the reacting Cl atom is nearer the central carbon atom than the terminal one of propene.

When a *p*-H_2 matrix containing Cl_2 and *trans*-1,3-butadiene in small proportions was irradiated with light at 365 nm, intense lines at 646.7, 809.0, 962.2, 1240.6 cm^{-1}, and several weaker ones assigned to the *trans*-1-chloromethylallyl radical, $^{\bullet}(CH_2CHCH)CH_2Cl$, appeared.[65] That the Cl atom adds primarily to the terminal carbon atom of *trans*-1,3-butadiene is in agreement with the path of minimum energy predicted quantum-chemically.

The reaction of a Cl atom with benzene (C_6H_6) is very important in organic chemistry, especially in site-selective chlorination reactions in benzene solvent, but whether its product Cl–C_6H_6 complex has a π- or σ-form has been a subject of debate for five decades.[67] Upon photolysis at 365 nm of a Cl_2/C_6H_6 (or C_6D_6)/*p*-H_2 matrix, the IR spectrum, showing intense lines at 1430.5, 833.6, 719.8, 617.0, 577.4 cm^{-1} and several weaker ones, and the deuterium shifts of observed new lines support unambiguously that the product is a 6-chlorocyclohexadienyl radical, *i.e.*, the σ-complex of Cl–C_6H_6.[66] Observation of the σ-complex rather than the π-complex indicates that the σ-complex is more stable in solid *p*-H_2 at 3.2 K. The spectral information is crucial for further investigations of the Cl + C_6H_6 reaction in either the gaseous or solution phase.

The reaction of Cl + C_2H_2 in solid *p*-H_2 is expected to produce the 2-chlorovinyl ($^{\bullet}$CHCHCl) radical. However, upon addition of H to C_2H_2, $^{\bullet}$CHCHCl reacts readily with a neighbouring *p*-H_2 molecule to form $^{\bullet}CHClCH_3$ and C_2H_3Cl,[68] to be discussed in more detail in Section 6.1.

We compare the representative absorption lines of these radicals of the Cl + unsaturated hydrocarbon reactions in Table 1. The C–Cl stretching wavenumbers are similar in all three radicals, but the patterns of other absorption lines are quite distinct for each one because the bonding is different in each case.

Table 1 Vibrational wavenumbers/cm^{-1} and relative intensities of representative lines of free radicals produced from Cl + unsaturated hydrocarbons

Mode[a]	Cl + C_2H_4 → $^{\bullet}CH_2CH_2Cl$	Cl + C_3H_6 → $^{\bullet}CH_2CHClCH_3$	Cl + C_4H_6 → $^{\bullet}(C_3H_4)CH_2Cl$
C–Cl str.	664.0 (100)[b]	649.9 (100)[b]	650.3 (37)[b]
$C_{Cl}H_2$ rock			870.5 (3)
CH_3 rock		1007.6 (19)	
ClCH b.		1149.6 (31)	
		1214.7 (10)	
CH_3 def.		1382.2 (16)	
$C_{Cl}H_2$ w.	1228.0 (13)		1240.6 (38)
$C_{Cl}H_2$ sci.			1442.6 (4)
$C_{Cl}H_2$ str.			2962.3 (19)
$^{\bullet}CH_2$ s. str.	3041.1 (6)		
$^{\bullet}CH_2$ as. str.	3129.3 (4)		3112.8 (18)
Ref.	63	64	65

[a] s.: symmetric; as.: antisymmetric; str.: stretch; b.: bend; r.: rock; t.: twist; w.: wag; sci.: scissor; def.: deformation. [b] Integrated IR intensity relative to the most intense line observed for each species.

4.2 Reactions of free radicals

In addition to atoms, a bimolecular reaction can also involve a free radical; the reaction of CH_3 + SO_2 is an example. Irradiation with a mercury lamp at 254 nm of a *p*-H_2 matrix containing CH_3I and SO_2 at 3.3 K, followed by annealing of the matrix, produced prominent features at 633.8, 917.5, 1071.1, 1272.5, and 1416.0 cm^{-1}, attributed to ν_{11} (C–S stretching), ν_{10} (CH_3 wagging), ν_8 (SO_2 symmetric stretching), ν_7 (SO_2 antisymmetric stretching), and ν_4 (CH_2 scissoring) modes of CH_3SO_2, respectively.[69] These assignments are based on a comparison of observed vibrational wavenumbers and ^{18}O- and ^{34}S-isotopic shifts with those predicted using the B3P86 method. These results also agree with the previously reported transient IR absorption bands of gaseous CH_3SO_2 at 1280 and 1076 cm^{-1},[70] but extend the number of observed lines to 5, including the important C–S stretching mode.

Hoshina *et al.* irradiated dimers or larger clusters of C_2H_2 in solid *p*-H_2 with light at 193 nm and observed IR absorption of C_3, C_5, and C_7, along with those of CH_4, C_2H_4, C_2H_5, C_2H_6, and C_4H_2.[71] In contrast, the photolysis of C_2H_4 dimers and trimers in a Xe matrix with 193 nm irradiation yielded mainly butadiyne (C_4H_2) with ethene (C_2H_4), 1,3-butadiene (C_4H_6), and butenyne (C_4H_4, vinylacetylene) as byproducts.[72]

4.3 Reactions of a secondary H atom

Raston and Anderson reported that Cl atoms reacted with *p*-H_2 readily to form HCl, even when the matrix was irradiated only with IR light while recording the IR spectrum.[73] They further investigated the system with IR + UV irradiation and found evidence for translationally hot Cl atoms (Cl*) playing a significant role in the Cl + H_2 ($\nu = 1$) → HCl + H reaction.[74] This reaction of Cl + H_2 ($\nu = 1$) becomes an excellent method to produce H atoms for further reactions. Because of the diffusion of H atoms in solid *p*-H_2, reactions of H with other molecules are facile even at temperature below 2 K.[75] The delocalization nature of H atoms makes the reactions of H atoms quite unique and deserves further investigation.

When the UV-irradiated Cl_2/*trans*-1,3-butadiene/*p*-H_2 matrix was further irradiated with IR light from the FTIR spectrometer, intense lines at 781.6, 957.9, 1433.6, 2968.8, 3023.5, and 3107.3 cm^{-1} appeared and were assigned to the *trans*-1-methylallyl radical, $^{\bullet}(CH_2CHCH)CH_3$, produced from reaction of 1,3-butadiene with an H atom.[65]

Similar techniques were applied to obtain IR spectra of C_5H_5NH and 4-C_5H_6N.[76] The formation of C_5H_5NH is consistent with quantum-chemical computations that predict it to be the most stable among all isomers, whereas the formation of 4-C_5H_6N but not 2-C_5H_6N or 3-C_5H_6N is inexplicable with the barriers and enthalpies of formation of possible reactions predicted quantum-chemically, because the corresponding values for formation of 4-C_5H_6N are slightly greater than those

of 2-C_5H_6N and 3-C_5H_6N. One possible explanation is that the charge density over the C4 atom is more negative than those of the C2 and C3 atoms, so that the H atom might attack C4 more favourably. More sophisticated computations are required to explain the observed selectivity.

The H atoms can also be produced from other methods such as photofragmentation of NH_3 (ref. 54) and photolysis of N_2O;[77] the latter generates $O(^1D)$ that reacts readily with *p*-H_2 to form OH and the H atom. Anderson investigated the reactions H + NO and H + N_2O and observed IR absorption of HNO/HON[78] and *cis*-/*trans*-HNNO,[77] respectively. They also found that the rate of the H + NO reaction shows Arrhenius-like behavior whereas that of the H + N_2O reaction shows pronounced non-Arrhenius behavior. Further investigations are required to understand the mechanism of H-atom diffusion and reaction.

5. Production of protonated species and their neutrals

A new application of the *p*-H_2 matrix isolation technique to produce protonated species and their neutral counterparts has recently been developed in our laboratory. In this method, we applied an electron gun to bombard the *p*-H_2 matrix during deposition. Ionization of H_2 by electron impact produced H_2^+; subsequent rapid exothermic proton transfer of H_2^+ to H_2 produced H and H_3^+.[79] The H_3^+ thus produced can readily transfer a proton to a guest molecule to form a protonated species. Neutralization of the protonated species or the reaction of an H atom with a guest molecule produced the neutral counterpart of the protonated species, the mono-hydrogenated compound. These reactions are believed to occur mainly on the surface of *p*-H_2 because electron bombardment after deposition produced much less protonated species. To distinguish the cationic and the neutral species is easy: maintaining the electron-bombarded matrix in darkness for a long period or irradiating the matrix with UV light to release trapped electrons can diminish the protonated species and produce its neutral counterpart; the UV irradiation might also induce unwanted photodissociation or isomerization. Secondary photolysis at varied wavelengths may be employed to distinguish further the groups of lines associated with varied carriers.

5.1 Protonated PAH (polycyclic aromatic hydrocarbons)

The so-called unidentified interstellar infrared (UIR) bands of galactic and extragalactic objects show emission features at 3.3, 6.2, 7.7, 8.6, and 11.2 μm.[80] These features are generally attributed to polycyclic aromatic hydrocarbons (PAH) and their derivatives,[81] even though no PAH responsible for the UIR bands has been definitively identified. Because proton sources are abundant in space, protonated PAH, designated H^+PAH, are expected to be likewise abundant. H^+PAH are candidates for carriers of the UIR bands from the perspective of interstellar chemistry because they are stable closed-shell molecules.[82] It is hence important to record IR spectra of H^+PAH in laboratories for comparison with UIR bands. Recording IR spectra of H^+PAH in laboratories is challenging, however, largely because generating H^+PAH in a sufficient quantity for spectral interrogation is difficult. Two major spectral methods have been employed to yield IR spectra of H^+PAH: one employed IR multiphoton dissociation (IRMPD) of H^+PAH maintained in an ion trap, but the bands are typically broad and red-shifted;[83,84] another measured the single-photon IR photodissociation (IRPD) action spectrum of jet-cooled H^+PAH tagged with a weakly bound ligand, such as Ar, but tagging the large PAH is difficult because of the large internal energy of PAH.[85,86] Our method, being relatively clean with negligible fragmentation, is applicable to larger H^+PAH; its advantages are the production of IR spectra covering a broad spectral range with narrow lines and accurate IR intensities.

Using this technique, we have recorded high-resolution IR absorption spectra of H^+PAH according to the evolution of the circumferential growth of peri-condensed PAH, from protonated forms of benzene ($C_6H_7^+$),[87] naphthalene (1- and 2-$C_{10}H_9^+$),[88] pyrene (1-$C_{16}H_{11}^+$),[89] to coronene (1-$C_{24}H_{13}^+$).[90] The narrow widths of the lines enabled us to distinguish clearly between isomers 1-$C_{10}H_9^+$ and 2-$C_{10}H_9^+$; 2-$C_{10}H_9^+$ was unstable and converted to 1-$C_{10}H_9^+$ in less than 30 min.

Fig. 3 compares the IR absorption spectra of protonated pyrene (trace c) and coronene (trace d) isolated in solid *p*-H_2 with those recorded using the IRMPD method (traces a and b) and the UIR spectrum (trace e) of the photodissociation region at the Orion Bar.[81] The significant superiority of the spectra recorded using our technique to those of the IRMPD method is demonstrated. A survey of these experimental results shows that all these protonated species have IR features near 6.2 μm, characteristic of the C=C stretching mode of aromatic rings, which do not shift as the size increases. Three major lines in the 7–9 μm region are red-shifted from 7.19, 7.45, and 8.13 μm of 1-$C_{16}H_{11}^+$ to 7.37, 7.53, and 8.21 μm of 1-$C_{24}H_{13}^+$, showing the direction towards the UIR bands near 7.6, 7.8, and 8.6 μm.

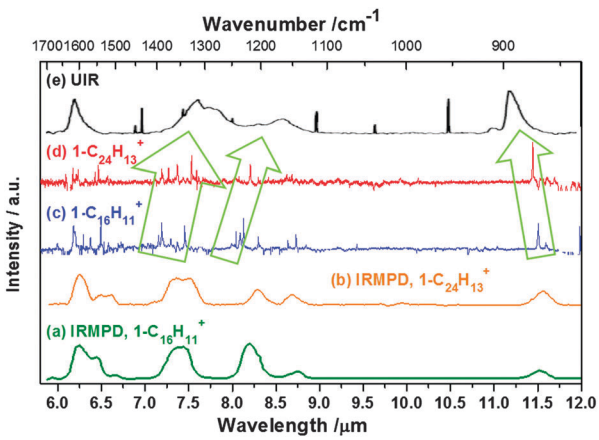

Fig. 3 Comparison of IR spectra of protonated pyrene and coronene with UIR bands. (a) IRMPD spectrum of protonated pyrene (1-$C_{16}H_{11}^+$);[83] (b) IRMPD spectrum of protonated coronene ($C_{24}H_{13}^+$);[83] (c) IR spectrum of 1-$C_{16}H_{11}^+$ in solid *p*-H_2;[89] (d) IR spectrum of $C_{24}H_{13}^+$ in solid *p*-H_2;[90] (e) UIR spectrum observed in Orion, adapted from ref. 81. The light green arrows indicate the trends of spectral shifts.

These three modes correspond to the ring deformation, CH_2 scissoring, and in-plane CH bending modes, respectively; the second one of these is unique and characteristic of H^+PAH. In contrast, the line at 11.5 μm for out-of-plane CH bending mode of 1-$C_{16}H_{11}^+$ is blue-shifted to 11.4 μm for 1-$C_{24}H_{13}^+$, showing the direction toward the UIR band near 11.2 μm. The IR features of protonated pyrene and coronene collectively appear to have the required chromophores for the prominent features of the UIR bands, and the spectral shifts as the circumference of aromatic rings increases point the appropriate direction toward the positions of the UIR bands. Larger protonated peri-condensed PAH might thus be important species among the carriers of UIR bands.

5.2 Other protonated species

This technique is not limited to protonation of PAH. We have recorded the IR absorption spectra of 1-pyridinium ($C_5H_5NH^+$) cation upon electron bombardment during matrix deposition of a mixture of pyridine (C_5H_5N) and p-H_2.[76] $C_5H_5NH^+$ was the most stable of four possible isomers of $C_5H_6N^+$ and its isolated spectrum has not been reported previously.

However, preliminary attempts to investigate the IR spectrum of $C_2H_5^+$ and $C_2H_3^+$ from electron bombardment of C_2H_4 and C_2H_2 in p-H_2 were unsuccessful because further fragmentation and reaction of the species of interest occurred. Apparently the proton affinity and the stability of the protonated species should be considered in the application of this technique.

Some preliminary results indicate that this technique is also useful in the investigation of protonated amino acids or other biomolecules, especially those that have more than one site to compete for protons. The IR spectra of each protonated isomer provide definitive information for structural identification and for future direct probes.

5.3 Mono-hydrogenated PAH

The method is also ideal for studying neutral HPAH, which are difficult to produce cleanly in the gaseous phase because the secondary reactions hamper the control of the extent of hydrogenation. Typically, only mono-hydrogenated species were produced using this technique, as shown in IR spectra of C_6H_7,[87] 1-$C_{10}H_9$,[88] 2-$C_{10}H_9$,[88] 1-$C_{16}H_{11}$,[89] 1-$C_{24}H_{13}$,[90] C_5H_5NH, and 4-C_5H_6N;[76] all IR spectra except C_6H_7 were previously unobserved, and many more lines of C_6H_7 than in previous reports were observed. The electronic transitions of 1-$C_{16}H_{11}$ and 1-$C_{24}H_{13}$ might play a role in the diffuse interstellar bands (DIB).[91]

The technique of generating H atoms *via* UV irradiation followed by IR irradiation of a p-H_2 matrix containing Cl_2 in a small proportion and a second guest species, discussed in Section 4.3, is also suitable for generating mono-hydrogenated PAH to assist the spectral assignments; examples of C_5H_5NH and 4-C_5H_6N,[76] and mono-hydrogenated coronene (1-$C_{24}H_{13}$)[90] have been demonstrated to be produced with both methods.

6. Limitations in using p-H_2

Even though the use of p-H_2 makes the photolytic production of free radicals much easier than with noble-gas matrix hosts, it still has some limitations. Some of them are general for matrix-isolation techniques, but some are inherent to the properties of p-H_2.

When one uses photodissociation to generate atoms or free radicals in matrices, the secondary photolysis might cause complications when the species of interest is photodissociated by light of the same wavelength. For example, when we applied light at 365 nm or 355 nm to irradiate a p-H_2 matrix containing Cl_2 and CS_2 in small proportions, absorption lines of only CS and Cl were observed because the primary product ClSCS absorbs strongly near this region to produce Cl + CS_2 and ClS + CS.[34] To observe the IR spectrum of ClSCS we selected light at 340 nm to dissociate Cl_2 but not ClSCS.

Extreme caution is necessary when one tries to derive a photolytic mechanism based on the observed spectra of products, because the secondary photolysis and the matrix cage effect might interfere. The temporal evolution profiles of each species might provide some insight into the mechanism. Otherwise, comparison of the results of photolysis in solid p-H_2 with those for noble-gas matrices might clarify processes due to the matrix cage effect. For example, the photolysis of CH_3SSCH_3 in solid p-H_2 at 248 nm produced mainly CH_3 and CH_3S, indicating that the main products CH_3SH and H_2CS observed in photolysis of CH_3SSCH_3 in solid Ar were due to secondary reactions in the original cage.[8]

6.1 Reactivity of p-H_2

The p-H_2 host is less inert than noble-gas hosts even at 2 K. If the photofragment carries sufficient energy to overcome the reaction barrier, reactions might occur. Fushitani *et al.* reported that irradiation of a CH_3I/p-H_2 matrix with light at 253.7 nm produced only the CH_3 radical, whereas light at 184.9 nm yielded both CH_3 radical and CH_4.[92] These authors concluded that CH_3 in the ground state did not react with p-H_2, but CH_3 in electronic excited state B $^2A_1'$, accessible on absorption of light at 184.9 nm, decomposed to a singlet methylene CH_2 (a $^1A_1$) and a H atom; the former reacted with p-H_2 to give CH_4. The nuclear spin selection rule for formation of CH_4 in this reaction has also been investigated.[93]

Another example is the reaction of Cl + C_2H_2 in solid p-H_2.[68] Instead of observing the expected primary addition product 2-chlorovinyl ($^\bullet$CHCHCl) radical, IR lines of the 1-chloroethyl radical ($^\bullet$CHClCH$_3$) and chloroethene (C_2H_3Cl) were identified as the main products upon irradiation of a Cl_2/C_2H_2/p-H_2 matrix with light at 365 nm. This observation indicates that, upon addition of H to C_2H_2, $^\bullet$CHCHCl reacted readily with a neighbouring p-H_2 molecule to form $^\bullet$CHClCH$_3$ and C_2H_3Cl. Observation of lines due to the $^\bullet$CDClCH$_2$D radical and *trans*-CHDCDCl from the reaction of Cl + C_2D_2 further supports this mechanism. For the same reason, when we tried to photolyze vinyl chloride (C_2H_3Cl) in solid p-H_2, we observed lines of only C_2H_5 instead of the vinyl (C_2H_3) radical even though C_2H_3

is the primary photolysis product; the energetic C_2H_3 upon photolysis reacted readily with p-H_2 to form C_2H_5.[94]

Momose *et al.* reported that the tunnelling reaction of CD_3 + H_2 → CD_3H + H occurred, but the corresponding reaction of CH_3 + H_2 was unobserved; the distinct behaviour between these two systems is attributed to the difference in the change of zero-point energies.[95] A further study of the reactions R + H_2 → RH + H (R = CD_3, CD_2H, CDH_2) indicated that the tunneling rate coefficient depends on the degree of deuteration, with k = 3.3 × 10^{-6}, 2.0 × 10^{-6}, and 1.0 × 10^{-6} s^{-1} for reactions of CD_3, CD_2H, and CDH_2, respectively, with H_2.[96]

Ruzi and Anderson reported that NH_2 was produced from NH_3 photolysis at 193 nm, but it undergoes a facile tunnelling-driven reaction with p-H_2 to form o-NH_3 and H with a lifetime of ~22 s.[54] The photo-produced o-NH_3 is created in a defect site, with o-NH_3 next to a nearest-neighbour vacancy or H-atom and is characterized by two satellite peaks on each side of the line for stable NH_3, and undergoes slow reversion to the more stable single substitution site even at 1.8 K. The production of satellite peaks due to the reaction of one photoproduct with the p-H_2 host was also observed for H_2O and HOD.[97,98]

Our preliminary work on IR spectra of CH_3O (CD_3O) produced from photolysis of CH_3ONO/p-H_2 (CD_3ONO/p-H_2) also indicates that CH_3O (CD_3O) reacts readily with p-H_2 to form CH_2OH (CD_2OH) within 10 min. Because the reaction of CH_3O (CD_3O) with H_2 has a barrier of ~5000 cm^{-1},[99] this reaction at 3 K must proceed *via* a tunnelling reaction.

IR irradiation of p-H_2 might also promote reactions. As discussed in Section 4.3, irradiation of light of wavelength smaller than 2.5 μm (4000 cm^{-1}) initiates the reaction Cl + H_2.[73,74] Our preliminary results obtained on using light from a tunable IR laser indicate that excitation of either the phonon band $Q_R(0)$ of solid p-H_2 or the Cl-perturbed H_2 absorption band $Q_1(0)$ can initiate the Cl + H_2 reaction. Similar results for excitation of the $S_R(0)$ and $S_1(0)$ bands were also observed. Excitation of the phonon bands is delocalized so that the exciton moves through the lattice to find a Cl atom for reaction, whereas excitation of the Cl-perturbed bands is localized, and the reaction only takes place in the specific excited Cl–H_2 complex.

6.2 Rapid energy relaxation

The rapid relaxation of the energy of photofragments or reaction products in solid p-H_2 is typically advantageous for the stabilization and preservation of free radicals produced upon irradiation. However, in some special cases in which secondary decomposition is required to prepare the free radical, the rapid relaxation might become disadvantageous. An example is the formation of the simplest Criegee intermediate, formaldehyde oxide (CH_2OO), an extremely important intermediate in the reaction of ozone with unsaturated hydrocarbons in the atmosphere.[100,101] An efficient scheme for the production of CH_2OO in the gaseous phase is UV photolysis of a mixture of CH_2I_2 and O_2;[102,103] the photofragment CH_2I reacts readily with O_2 to form CH_2OO + I. In contrast, when we irradiated a p-H_2 matrix containing CH_2I_2 and O_2 in small proportions with light at 309 nm, we observed only the stabilized adduct CH_2IOO instead of CH_2OO. A comparison of an IR spectrum of gaseous CH_2OO (trace a) with that obtained on irradiation of a CH_2I_2/O_2/p-H_2 matrix (trace c) is shown in Fig. 4; the spectra simulated according to quantum-chemical calculations are shown in traces b and d for comparison. Apparently the rapid energy relaxation in p-H_2 stabilizes the adduct CH_2IOO efficiently so that it has insufficient energy to break the C–I bond to form CH_2OO as in the gaseous phase.

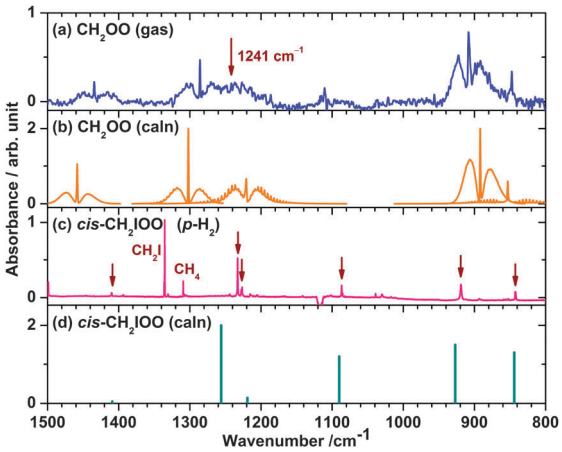

Fig. 4 Comparison of IR spectra of reaction products of CH_2I + O_2 in the gaseous phase and in a p-H_2 matrix. (a) Gaseous CH_2I_2 + O_2 irradiated with laser light at 248 nm; observed lines are due to CH_2OO and the band near 1100 cm^{-1} are due to interference of parent absorption. (c) A CH_2I_2/O_2/p-H_2 (1/8/3000) annealed at 4.5 K for 45 min and irradiated with light at 309 nm for 8 h. Lines marked with arrows are due to CH_2IOO. The corresponding quantum-chemical predictions for spectra of CH_2OO and CH_2IOO are shown in (b) and (d), respectively.

7. Concluding remarks and future aspects

p-H_2 is distinct from the noble gases as a matrix host. The small heterogeneous broadening yields spectral lines with small width. The diminished cage effect makes feasible the production of free radicals *via* direct photolysis *in situ* or from bimolecular reactions initiated with photodissociation. The application of p-H_2 as a novel matrix host has opened a new paradigm to produce unstable species that are difficult to prepare in noble-gas matrices. Nearly all spectra of the unstable species discussed in this paper are new.

The novel application of electron bombardment during the deposition of a p-H_2 matrix to produce protonated species and their neutral counterparts has several advantages over existing methods such as IR multiphoton dissociation of protonated species and IR photodissociation of Ar-tagged species. This technique, applicable to larger PAH and biomolecules, is clean with negligible fragmentation. It produces excellent IR spectra covering a broad spectral range with narrow lines and excellent signal to noise ratio; it is also the only existing method that provides accurate IR intensities.

Using p-H_2 as a matrix host has some limitations. The reactivity of p-H_2, including the tunnelling reactions and reactions activated with infrared radiation, sometimes limits the species that can be prepared *via* photolysis. Although not discussed in this paper, the interference of spectral lines due to the *fcc* crystal structure of p-H_2 and interaction of the guest species with o-H_2 impurity might complicate the spectra in some cases.[19]

Several new directions related to matrix-isolated free radicals await further exploration. For example, a complex of Cl (or other atom or radical) with a molecule X of interest can be formed on annealing the UV-irradiated p-H_2 matrix containing Cl_2 (or appropriate precursors) and X in small proportions. Excitation of this complex with tunable IR light might provide valuable information on the specificity of vibrational and rotational excitation of X, without interference from translational energy, in regard to chemical reaction dynamics. This study of 'chemical dynamics without translational energy' will be complementary to dynamical investigations using a cross-molecular beam with significant translational energy.

The electronic transitions of guest molecules isolated in solid p-H_2 are little investigated. The effects of p-H_2 on zero-phonon lines, phonon bands, selection rules, types of transition, and electronic energy relaxation need to be investigated in detail. Nonetheless, the ability to prepare numerous new free radicals that are difficult in noble-gas matrices or in the gaseous phase enables us to explore their electronic transitions.

Many fundamental issues remain little understood. The energy dissipation upon photoexcitation or photofragmentation, the diffusion dynamics of electrons, H atoms, and the photofragments, a convenient and definitive method for spectral identification of H atoms and electrons in solid p-H_2, and the tunnelling reactions and their temperature dependence also require further investigations.

Acknowledgements

The National Science Council of Taiwan (grants NSC102-2745-M-009-001-ASP) and the Ministry of Education, Taiwan (''ATU Plan'' of National Chiao Tung University) supported this work. The National Center for High-Performance Computing provided computer time.

Notes and references

1 E. Whittle, D. A. Dows and G. C. Pimentel, *J. Chem. Phys.*, 1954, **22**, 1943.
2 H. E. Hallam, *Vibrational Spectroscopy of Trapped Species*, Wiley, New York, USA, 1973.
3 M. Moskovits and G. A. Ozin, *Cryochemistry*, Wiley, New York, USA, 1976.
4 L. Andrews and M. Moskovits, *Chemistry and Physics of Matrix-Isolated Species*, North-Holland, Amsterdam, Netherlands, 1989.
5 M. J. Almond and A. J. Downs, *Advances in Spectroscopy*, Wiley, New York, USA, vol. 17, 1989.
6 M. E. Jacox, *J. Mol. Spectrosc.*, 1985, **113**, 286.
7 N. Pietri, M. Monnier and J.-P. Aycard, *J. Org. Chem.*, 1998, **63**, 2462.
8 M. Bahou and Y.-P. Lee, *J. Chem. Phys.*, 2010, **133**, 164316.
9 B.-M. Cheng, J.-W. Lee and Y.-P. Lee, *J. Phys. Chem.*, 1991, **95**, 2814.
10 W.-J. Lo and Y.-P. Lee, *J. Chem. Phys.*, 1994, **101**, 5494.
11 M. Bahou, Y.-C. Lee and Y.-P. Lee, *J. Am. Chem. Soc.*, 2000, **122**, 661.
12 L.-S. Chen, C.-I. Lee and Y.-P. Lee, *J. Chem. Phys.*, 1996, **105**, 9454.
13 Y.-P. Lee, *J. Chin. Chem. Soc.*, 1992, **39**, 503.
14 Y.-P. Lee, *J. Chin. Chem. Soc.*, 2005, **52**, 641.
15 T. Oka, *Annu. Rev. Phys. Chem.*, 1993, **44**, 299.
16 T. Momose and T. Shida, *Bull. Chem. Soc. Jpn.*, 1998, **71**, 1.
17 T. Momose, M. Fushitani and H. Hoshina, *Int. Rev. Phys. Chem.*, 2005, **24**, 533.
18 K. Yoshioka, P. L. Raston and D. T. Anderson, *Int. Rev. Phys. Chem.*, 2006, **25**, 469.
19 M. Bahou, C.-W. Huang, Y.-L. Huang, J. Glatthaar and Y.-P. Lee, *J. Chin. Chem. Soc.*, 2010, **57**, 771.
20 M. E. Fajardo, *Physics and Chemistry at Low Temperatures*, ed. L. Khriachtchev, Pan Stanford Publishing Pte. Ltd., Singapore, 2011, p. 167.
21 L. Andrews and X. Wang, *Science*, 2003, **229**, 2049.
22 J. V. Kranendonk, *Solid Hydrogen: Theory of the Properties of Solid H_2, HD and D_2, Plenum, New York, USA, 1983.*
23 S. Tam, M. E. Fajardo, H. Katsuki, H. Hoshina, T. Wakabayashi and T. Momose, *J. Chem. Phys.*, 1999, **111**, 4191.
24 T. Momose, M. Miki, T. Wakabayashi, T. Shida, M.-H. Chan, S. S. Lee and T. Oka, *J. Chem. Phys.*, 1997, **107**, 7707.
25 S. Tam and M. E. Fajardo, *J. Low Temp. Phys.*, 2001, **122**, 345.
26 M. E. Fajardo, C. M. Lindsay and T. Momose, *J. Chem. Phys.*, 2009, **130**, 244508.
27 M. E. Fajardo, S. Tam and M. E. DeRose, *J. Mol. Struct.*, 2004, **695**, 111.
28 D. T. Anderson, R. J. Hinde, S. Tam and M. E. Fajardo, *Chem. Phys. Lett.*, 2002, **356**, 355.
29 Y.-P. Lee, Y.-J. Wu, R. M. Lees, L.-H. Xu and J. T. Hougen, *Science*, 2006, **311**, 365.
30 Y.-P. Lee, Y.-J. Wu and J. T. Hougen, *J. Chem. Phys.*, 2008, **129**, 104502.
31 Y. A. Tobón, R. M. Romano, C. O. Della Védova and A. J. Downs, *Inorg. Chem.*, 2007, **46**, 4692.
32 R. M. Romano, C. O. Della Védova and A. J. Downs, *Chem. Commun.*, 2001, 2638.
33 Y. A. Tobón, L. I. Nieto, R. M. Romano, C. O. Della Védova and A. J. Downs, *J. Phys. Chem. A*, 2006, **110**, 2674.
34 C.-W. Huang, Y.-C. Lee and Y.-P. Lee, *J. Chem. Phys.*, 2010, **132**, 164303.
35 T. Momose, M. Miki, M. Uchida, T. Shimizu, I. Yoshizawa and T. Shida, *J. Chem. Phys.*, 1995, **103**, 1400.
36 T. Momose, M. Uchida, N. Sogoshi, M. Miki, S. Masuda and T. Shida, *Chem. Phys. Lett.*, 1995, **246**, 583.

37 N. Sogoshi, T. Wakabayashi, T. Momose and T. Shida, *J. Phys. Chem. A*, 1997, **101**, 522.
38 N. Sogoshi, T. Wakabayashi, T. Momose and T. Shida, *J. Phys. Chem. A*, 2001, **105**, 3077.
39 S. Tam and M. E. Fajardo, *Rev. Sci. Instrum.*, 1999, **70**, 1926.
40 B. A. Tom, S. Bhasker, Y. Miyamoto, T. Momose and B. J. McCall, *Rev. Sci. Instrum.*, 2009, **80**, 016108.
41 L. Andrews and X. Wang, *Rev. Sci. Instrum.*, 2004, **75**, 3039.
42 P. L. Raston and D. T. Anderson, *J. Chem. Phys.*, 2007, **126**, 021106.
43 S. C. Kettwich, L. O. Paulson, P. L. Raston and D. T. Anderson, *J. Phys. Chem. A*, 2008, **112**, 11153.
44 P. L. Raston, S. C. Kettwich and D. T. Anderson, *J. Chem. Phys.*, 2013, **139**, 134304.
45 R. J. Hinde, *J. At., Mol., Opt. Phys.*, 2012, **2012**, 916510.
46 R. J. Hinde, *J. Chem. Phys.*, 2013, **139**, 134305.
47 M. Fushitani, T. Momose and T. Shida, *Chem. Phys. Lett.*, 2002, **356**, 375.
48 P. Das and Y.-P. Lee, *J. Chem. Phys.*, 2013, **139**, 084320.
49 Y.-F. Lee, L.-J. Kong and Y.-P. Lee, *J. Chem. Phys.*, 2012, **136**, 124510.
50 J.-D. Chen and Y.-P. Lee, *J. Chem. Phys.*, 2011, **134**, 094304.
51 M. Fushitani, Y. Miyamoto, H. Hoshina and T. Momose, *J. Phys. Chem. A*, 2007, **111**, 12629.
52 H. Hoshina, M. Fushitani and T. Momose, *J. Mol. Spectrosc.*, 2011, **268**, 164.
53 Y. Miyamoto, M. Tsubouchi and T. Momose, *J. Phys. Chem. A*, 2013, **117**, 9510.
54 M. Ruzi and D. T. Anderson, *J. Phys. Chem. A*, 2013, **117**, 13832.
55 A. V. Marenich and J. E. Boggs, *J. Phys. Chem. A*, 2004, **108**, 10594.
56 A. V. Marenich and J. E. Boggs, *J. Chem. Theory. Comput.*, 2005, **1**, 1162.
57 M. Ruzi and D. T. Anderson, *J. Chem. Phys.*, 2012, **137**, 194313.
58 C. J. Bennett, C. S. Jamieson, Y. Osamura and R. I. Kaiser, *Astrophys. J.*, 2005, **624**, 1097.
59 C. Anastasi and P. R. Maw, *J. Chem. Soc., Faraday Trans. 1*, 1982, 78–2423.
60 C. D. Bass and G. C. Pimentel, *J. Am. Chem. Soc.*, 1961, **83**, 3754.
61 P. Das, M. Bahou and Y.-P. Lee, *J. Chem. Phys.*, 2013, **138**, 054307.
62 S. Parveen and A. K. Chandra, *J. Phys. Chem. A*, 2009, **113**, 177.
63 J. C. Amicangelo, B. Golec, M. Bahou and Y.-P. Lee, *Phys. Chem. Chem. Phys.*, 2012, **14**, 1014.
64 J. C. Amicangelo and Y.-P. Lee, *J. Phys. Chem. Lett.*, 2010, **1**, 2956.
65 M. Bahou, J.-Y. Wu, K. Tanaka and Y.-P. Lee, *J. Chem. Phys.*, 2012, **137**, 084310.
66 M. Bahou, H. Witek and Y.-P. Lee, *J. Chem. Phys.*, 2013, **138**, 074310.
67 M.-L. Tsao, C. M. Hadad and M. S. Platz, *J. Am. Chem. Soc.*, 2003, **125**, 8390.
68 B. Golec and Y.-P. Lee, *J. Chem. Phys.*, 2011, **135**, 174302.
69 Y.-F. Lee and Y.-P. Lee, *J. Chem. Phys.*, 2011, **134**, 124314.
70 L.-K. Chu and Y.-P. Lee, *J. Chem. Phys.*, 2006, **124**, 244301.
71 H. Hoshina, Y. Kato, Y. Morisawa, T. Wakabayashi and T. Momose, *Chem. Phys.*, 2004, **300**, 69.
72 G. Maier and C. Lautz, *Eur. J. Org. Chem.*, 1998, 769.
73 P. L. Raston and D. T. Anderson, *Phys. Chem. Chem. Phys.*, 2006, **8**, 3124.
74 S. C. Kettwich, P. L. Raston and D. T. Anderson, *J. Phys. Chem. A*, 2009, **113**, 7621.
75 M. Fushitani and T. Momose, *Low Temp. Phys.*, 2003, **29**, 740. [*Fiz. Nizk. Temp.*, 2003, **29**, 985.].
76 B. Golec, P. Das, M. Bahou and Y.-P. Lee, *J. Phys. Chem. A*, 2013, **117**, 13680.
77 F. M. Mutunga, S. E. Follett and D. T. Anderson, *J. Chem. Phys.*, 2013, **139**, 151104.
78 M. Ruzi, F. M. Mutunga and D. T. Anderson, private communication.
79 M.-C. Chan, M. Okumura and T. Oka, *J. Phys. Chem. A*, 2000, **104**, 3775.
80 A. G. G. M. Tielens, *PAHs and the Universe*, ed. C. Joblin and A. G. G. M. Tielens, EAS Publication Series, 2011, vol. 46, p. 3.
81 E. Peeters, *PAHs and the Universe*, ed. C. Joblin and A. G. G. M. Tielens, EAS Publication Series, 2011, vol. 46, p. 13.
82 T. P. Snow, V. L. Page, Y. Keheyan and V. M. Bierbaum, *Nature*, 1998, **391**, 259.
83 O. Dopfer, *PAHs and the Universe*, ed. C. Joblin and A. G. G. M. Tielens, EAS Publication Series, 2011, vol. 46, p. 103.
84 H. Knorke, J. Langer, J. Oomens and O. Dopfer, *Astrophys. J., Lett.*, 2009, **706**, L66.
85 G. E. Douberly, A. M. Ricks, P. V. R. Schleyer and M. A. Duncan, *J. Phys. Chem. A*, 2008, **112**, 4869.
86 A. M. Ricks, G. E. Douberly and M. A. Duncan, *Astrophys. J.*, 2009, **702**, 301.
87 M. Bahou, Y.-J. Wu and Y.-P. Lee, *J. Chem. Phys.*, 2012, **136**, 154304.
88 M. Bahou, Y.-J. Wu and Y.-P. Lee, *Phys. Chem. Chem. Phys.*, 2013, **15**, 1907.
89 M. Bahou, Y.-J. Wu and Y.-P. Lee, *J. Phys. Chem. Lett.*, 2013, **4**, 1989.
90 M. Bahou, Y.-J. Wu and Y.-P. Lee, *Angew. Chem., Int. Ed.*, DOI: 10.1002/anie.201308971.
91 I. Garkusha, J. Fulara, P. J. Sarre and J. P. Maier, *J. Phys. Chem. A*, 2011, **115**, 10972.
92 M. Fushitani, N. Sogoshi and T. Wakabayashi, *J. Chem. Phys.*, 1998, **109**, 6346.
93 M. Fushitani and T. Momose, *J. Chem. Phys.*, 2002, **116**, 10739.
94 Y.-J. Wu, X. Yang and Y.-P. Lee, *J. Chem. Phys.*, 2004, **120**, 1168.
95 T. Momose, H. Hoshina, N. Sogoshi, H. Katsuki, T. Wakabayashi and T. Shida, *J. Chem. Phys.*, 1998, **108**, 7334.
96 H. Hoshina, M. Fushitani, T. Momose and T. Shida, *J. Chem. Phys.*, 2004, **120**, 3706.

97 W. R. Wonderly and D. T. Anderson, *Low Temp. Phys.*, 2012, **38**, 673.
98 K. A. Kufeld, W. R. Wonderly, L. O. Paulson, S. C. Kettwich and D. T. Anderson, *J. Phys. Chem. Lett.*, 2012, **3**, 342.
99 M.-P. Rubén, G. T. Donald and F.-R. Antonio, *J. Chem. Phys.*, 2011, **134**, 094302.
100 W. H. Bunnelle, *Chem. Rev.*, 1991, **91**, 335.
101 S. Hatakeyama and H. Akimoto, *Res. Chem. Intermed.*, 1994, **20**, 503.
102 O. Welz, J. D. Savee, D. L. Osborn, S. S. Vasu, C. J. Percival, D. E. Shallcross and C. A. Taatijes, *Science*, 2012, **335**, 204.
103 Y.-T. Su, Y.-H. Huang, H. A. Witek and Y.-P. Lee, *Science*, 2013, **340**, 174.

